Organic Electronics 14 (2013) 2424–2430

Contents lists available at SciVerse ScienceDirect

Organic Electronics

journal homepage: www.elsevier.com/locate/orgel

Improving device efficiencies of solid-state white light-emitting electrochemical cells by adjusting the emissive-layer thickness

Yuan-Pei Jhang [a], Hsiao-Fan Chen [b], Hung-Bao Wu [a], Yun-Shiuan Yeh [b], Hai-Ching Su [a,*], Ken-Tsung Wong [b,*]

[a] Institute of Lighting and Energy Photonics, National Chiao Tung University, Tainan 71150, Taiwan
[b] Department of Chemistry, National Taiwan University, Taipei 10617, Taiwan

ARTICLE INFO

Article history:
Available online 1 July 2013

Keywords:
Light-emitting electrochemical cells
Recombination zone
White light

ABSTRACT

Exciton quenching in the recombination zone close to electrochemically doped regions would be one of the bottlenecks for improving device efficiencies of solid-state white light-emitting electrochemical cells (LECs). To further enhance device efficiencies of white LECs for practical applications, we adjust the emissive-layer thickness to reduce exciton quenching. In white LECs with properly thickened emissive-layer thickness, the recombination zone can be situated near the center of the emissive layer, rendering mitigated exciton quenching and thus enhanced device efficiencies. High external quantum efficiencies and power efficiencies of optimized devices reach *ca.* 11% and 20 lm/W, respectively, which are among the highest reported for white LECs. These results confirm that tailoring the thickness of the emissive layer to avoid exciton quenching would be a feasible approach to improve device efficiencies of white LECs.

1. Introduction

Recently, white organic light-emitting diodes (OLEDs) have attracted intense attention due to their potential applications in flat-panel displays and solid-state lighting [1,2]. Compared with conventional OLEDs, solid-state light-emitting electrochemical cells (LECs) [3,4] possess several superior advantages. In LECs, electrochemically doped regions, i.e. p-type doping near the anode and n-type doping near the cathode, are formed by spatially separated ions under a bias. Such doped regions significantly reduce carrier injection barriers at electrodes, giving balanced carrier injection, low operating voltages, and consequently high power efficiencies. Therefore, LECs generally require only a single emissive layer, which can be easily deposited by solution processes and can conveniently utilize air-stable electrodes.

Some works of fluorescent solid-state white LECs based on conjugated polymers have been reported [5–9]. However, moderate device efficiencies of polymer white LECs showed that the fluorescent nature of conjugated polymers limits the eventual electroluminescence (EL) efficiency due to the spin statistics. To improve device efficiencies, phosphorescent cationic transition metal complexes (CTMCs) have been intensively studied for use in solid-state LECs [10–32]. By employing a blue-emitting host and a red-emitting guest, solid-state white LECs based on host-guest CTMCs have been demonstrated to exhibit efficient white EL emission [19,21,22,25,32] and an external quantum efficiency (EQE) up to *ca.* 8% was achieved [32]. Recently, blue-emitting LECs combined with red-emitting color conversion layers have also been shown to exhibit efficient white EL emission with an EQE of *ca.* 6% [29]. Further improvement in device efficiency is highly required for practical applications. In single-layered LECs, p-doped/intrinsic (undoped)/n-doped (p–i–n) structure is formed under electrical driving and the intrinsic layer thickness reduces due to extension of doped layers [27]. Electrochemically doped layers adjacent to the intrinsic emitting layer result

* Corresponding authors. Tel.: +886 6 3032121 57792; fax: +886 6 3032535 (H.-C. Su), tel.: +886 2 33661665; fax: +886 2 33661667 (K.-T. Wong).
E-mail addresses: haichingsu@mail.nctu.edu.tw (H.-C. Su), kenwong@ntu.edu.tw (K.-T. Wong).

1566-1199/$ - see front matter © 2013 Elsevier B.V. All rights reserved.
http://dx.doi.org/10.1016/j.orgel.2013.06.015

in exciton quenching as the intrinsic layer thickness decreases over time [27]. Thus, adjusting the thickness of the active layer for keeping the recombination zone away from doped layers would be a feasible way to mitigate exciton quenching and to improve device efficiency consequently. In this work, we compare EL characteristics of white LECs with various thicknesses of active layers and the corresponding recombination zone positions are estimated by employing microcavity effect, i.e., fitting the measured EL spectrum and the simulated one with properly adjusted recombination zone positions [33]. As compared to thinner devices (<200 nm), the recombination zones in thicker devices are closer to the center of the active layer, resulting in lesser exciton quenching. Hence, a high EQE of 11%, which is among the highest reported in white LECs, can be achieved in white LECs with an active-layer thickness of 270 nm. However, further increasing the active-layer thickness to 400 nm leads to deteriorated device efficiency. In such over-thick devices, off-center recombination zones, which may be attributed to modified carrier mobilities under lower electric fields, would induce severer exciton quenching and cause lower device efficiencies as well. These results show that optimizing the active-layer thickness to minimize exciton quenching in the proximity of the doped layers would be an effective way to improve device efficiencies of white LECs.

2. Experiment

2.1. Materials

The chemical structures of host (**1**) and guest (**2**) materials used in this study are shown in Fig. 1a. Both complexes were synthesized according to the procedures reported in the literatures [15,19]. The blue-emitting cationic Ir complex $[Ir(dfppz)_2(dtb\text{-}bpy)]^+(PF_6^-)$ (**1**) (where dfppz is 1-(2,4-difluorophenyl)pyrazole and dtb-bpy is [4,4′-di(tert-butyl)-2,2′-bipyridine]) reported previously by Tamayo et al. [15] was used as the host. Highly retained photoluminescence quantum yield of complex **1** in neat films (0.75) [25] in comparison with that in dilute solutions (1.00) [25] reveals reduced self-quenching in neat films possibly resulting from the sterically bulky di-*tert*-butyl groups of the bipyridine ligand [15], suggesting its suitability for use as the host material of white LECs. Furthermore, complex **1** also exhibits superior carrier balance and a high EQE > 14% was achieved in LECs based on complex **1** [29]. $[Ir(ppy)_2(biq)]^+(PF_6^-)$ (**2**) (where ppy is 2-phenylpyridine and biq is 2,2′-biquinoline), which was used as the red-emitting complex in white LECs reported by Su et al. [19], was utilized as the red-emitting guest. The energy level alignments (estimated by cyclic voltammetry) of the host and guest are shown in Fig. 1b [25]. The PL spectrum of host and the absorption spectrum of guest in dichloromethane solutions (10^{-5} M) are shown in Fig. 1c. The blue-emitting host exhibits PL emission centered at 490 nm. The guest possesses broad absorption band extending from ~400 nm to the emission band of host, facilitating Förster energy transfer from host to guest.

2.2. LEC device fabrication and characterization

Indium tin oxide (ITO)-coated glass substrates were cleaned and treated with UV/ozone prior to use. A thin poly(3,4-ethylenedioxythiophene):poly(styrene sulfonate) (PEDOT:PSS) layer (30 nm) was spin-coated at 4000 rpm onto the ITO substrate in air and baked at 150 °C for

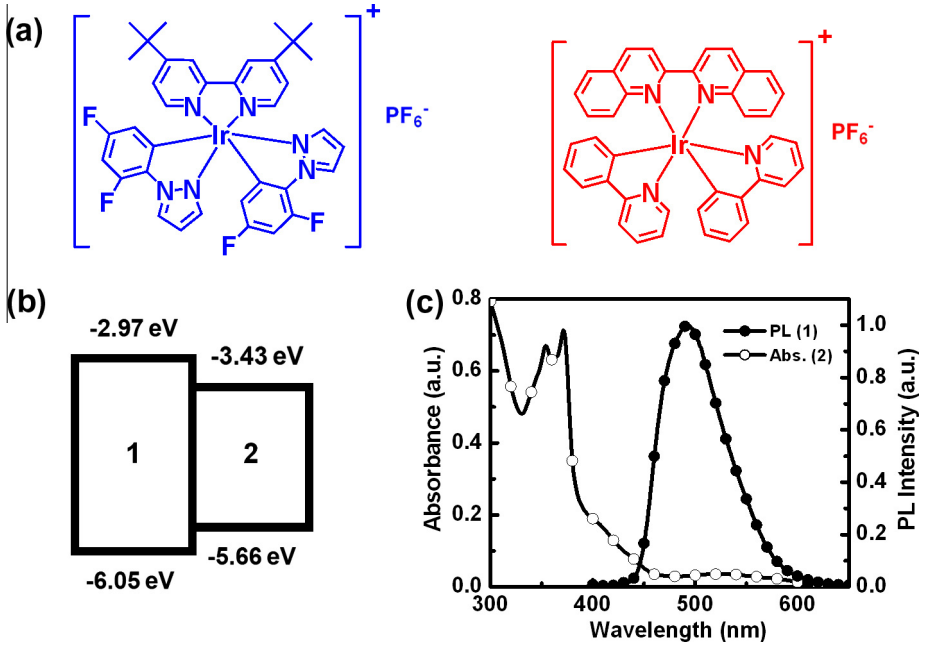

Fig. 1. (a) The molecular structures of host (**1**) and guest (**2**) materials, (b) the energy level diagram of **1** and **2** and (c) absorption spectrum of **2** and PL spectra of **1** in dichloromethane solutions (10^{-5} M).

30 min. The emissive layer contains **1** (79.85 wt.%), **2** (0.15 wt.%) and 1-butyl-3-methylimidazolium hexafluorophosphate [$BMIM^+(PF_6^-)$] (20 wt.%). The ionic liquid [$BMIM^+(PF_6^-)$] was added to enhance the ionic conductivity of thin films, resulting in reduced turn-on time of the LEC devices [13]. The concentrations of the solutions used for spin coating of the emissive layers for **Device I**, **II** and **III** are 120, 150 and 150 mg/mL, respectively. The emissive layers of **Device I**, **II** and **III** were spin-coated from the acetonitrile solutions under ambient conditions at 3000, 3000 and 1500 rpm, respectively. The thicknesses of the emissive layers for **Device I, II** and **III** are 190, 270 and 400 nm, respectively**.** After spin coating, the samples were then baked at 70 °C for 10 h in a nitrogen glove box, followed by thermal evaporation of a 100-nm Ag top contact in a vacuum chamber ($\sim 10^{-6}$ torr). Thicknesses of thin films were measured by profilometry. The electrical and emission characteristics of LEC devices were measured using a source-measurement unit and a Si photodiode calibrated with the Photo Research PR-650 spectroradiometer. All device measurements were performed under constant bias voltages (3.1, 3.3 and 3.5 V) in a nitrogen glove box. The EL spectra were taken with a calibrated CCD spectrograph.

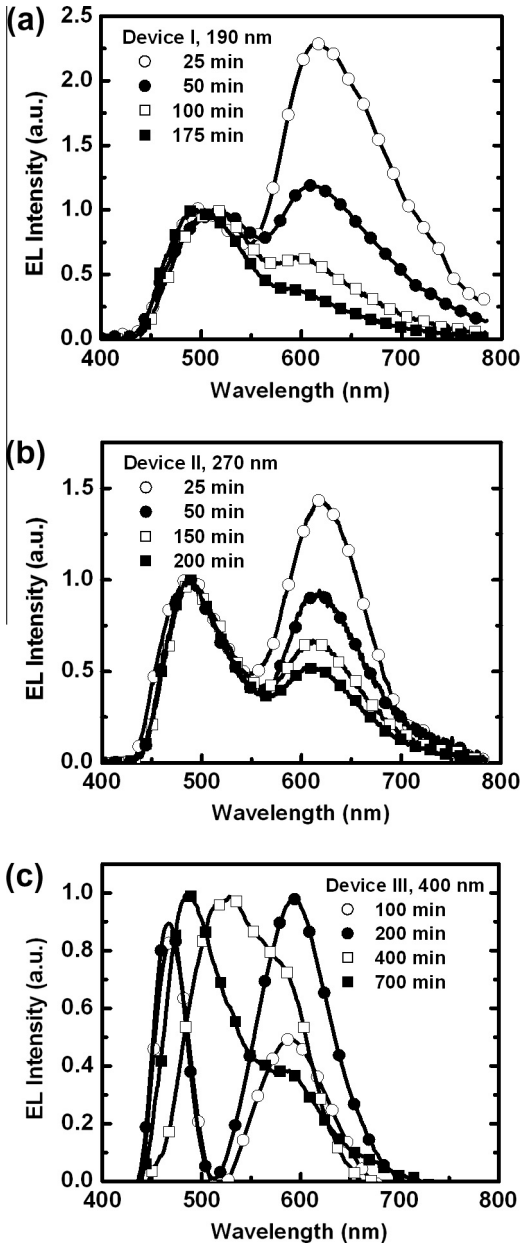

Fig. 2. Time dependent EL spectra of **Device** (a) **I**, (b) **II** and (c) **III** under 3.3 V.

3. Results and discussions

The time-dependent EL spectra of **Devices I**, **II** and **III** under 3.3 V are shown in Fig. 2a–c, respectively. As shown in Fig. 2a, for **Devices I**, the relative amount of red emission with respect to blue emission significantly decreased with time. It would be attributed to carrier trapping effect induced by the offsets between energy levels of host and guest molecules (Fig. 1b). In host–guest white LECs, both exciton formation on the host followed by host–guest energy transfer and direct exciton formation on the guest induced by carrier trapping contribute to the guest emission. At the early stage of operation, doped layers have not well established yet and high energy barriers for carrier injection into the host are still present. Such energy level alignments (Fig. 1b) favor carrier injection and trapping on the smaller-gap guests, resulting in direct carrier recombination/exciton formation on the guest (rather than host-guest energy transfer). Thus, red emission was more predominant during the initial 50-min operation (Fig. 2a). After the doped layers had been gradually formed, energy barriers for carrier injection into the host reduced significantly and exciton formation on the host and subsequent host-guest energy transfer dominated, rendering increased relative amount of blue emission with time. Finally, the EL spectra were approaching stable ($t > 175$ min) due to well established doper layers. EL spectra of **Device II** under 3.3 V also exhibited similar time-dependent evolution trend. However, slightly enhanced red emission as com-

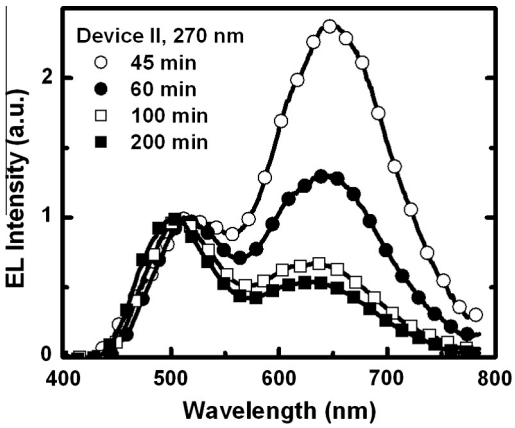

Fig. 3. Time dependent EL spectra of re-biased **Device II** under 3.3 V after a 24-hr idle time.

pared to blue emission was observed in thicker **Device II** (Fig. 2b). It results from a reduced electric field in a thicker device, which relatively facilitates direct exciton formation on the guest and thus more red emission is present. For **Device III**, the evolution of EL spectra is significantly different from that of **Devices I** or **II.** The blue emission peak was blue-shifted and the full width at half maximum (FWHM) was reduced at $t < 200$ min (Fig. 2c). Then the EL spectrum shifted to green region and the FWHM enhanced ($t = 400$ min, Fig. 2c). Finally, a white EL spectrum was reached but the relative amount of red emission was lower than that of **Devices I** or **II** ($t > 700$ min, Fig. 2c). This abnormal evolution phenomenon should not be attributed to carrier trapping effect since not only the relative amount of blue and red emission but also the FWHM of EL spectrum was significantly altered. It would be a typical feature of microcavity effect [34], which has also been observed in thicker LEC devices [32,33].

To examine the possibility of side reactions responsible for the time-dependent EL evolution, the time dependent EL spectra of re-biased **Device II** under 3.3 V after a 24-hr idle time were measured and are shown in Fig. 3. The EL evolution trend of the re-biased device is similar to that of the pristine device (*cf.* Figs. 3 and 2b). It reveals that side reactions would not be significant and the EL evolution shown in Fig. 2b mainly comes from carrier trapping effect.

The emission properties of the emissive layer can be modified in a microcavity structure, which alters the optical mode density within it and spectrally redistributes the EL spectrum. The output EL spectrum of a bottom emitting OLED device can be calculated approximately by using the following equation [34]:

$$|E_{ext}(\lambda)|^2 = \frac{T_2 \frac{1}{N}\sum_{i=1}^{N}\left[1 + R_1 + 2\sqrt{R_1}\cos\left(\frac{4\pi z_i}{\lambda} + \varphi_1\right)\right]}{1 + R_1 R_2 - 2\sqrt{R_1 R_2}\cos\left(\frac{4\pi L}{\lambda} + \varphi_1 + \varphi_2\right)} \times |E_{in_t}(\lambda)|^2$$

where R_1 and R_2 are the reflectance from the cathode and from the glass substrate, respectively, φ_1 and φ_2 are the phase changes on reflection from the cathode and from the glass substrate, respectively, T_2 is the transmittance from the glass substrate, L is the total optical thickness of the cavity layers, $|E_{in_t}(\lambda)|^2$ is the emission spectrum of the organic materials without alternation of the microcavity effect, $|E_{ext}(\lambda)|^2$ is the output emission spectrum from the glass substrate, z_i is the optical distance between the emitting sublayer i and the cathode. The emitting layer is divided into N sublayers and their contributions are summed up. Since the width of p–n junction estimated by capacitance measurements when p- and n-type layers were fully established was shown to be *ca.* 10% of the thickness of the active layer of LECs [35], the emitting layer width is estimated to be tenth of the active layer thickness. Thickness of each emitting sublayer of 1 nm was used and thus N = thickness of the active layer/10. The photoluminescence (PL) spectrum of a thin film of the emissive layer of white LECs coated on a quartz substrate was used as the emission spectrum without alternation of the microcavity effect since no highly reflective metal layer is present in this sample. Simulation was performed by implementing the equation shown above through the MATLAB codes.

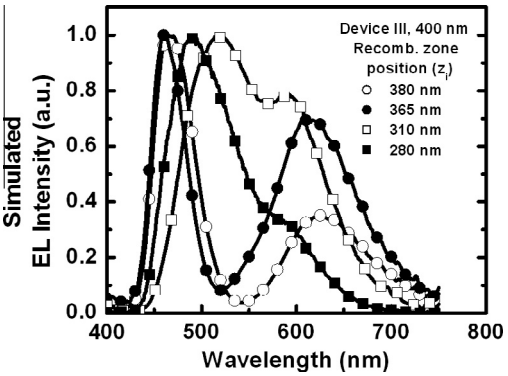

Fig. 4. Simulated output EL spectra of **Device III** when the recombination zone position, as measured from the cathode, varies from 380 to 280 nm.

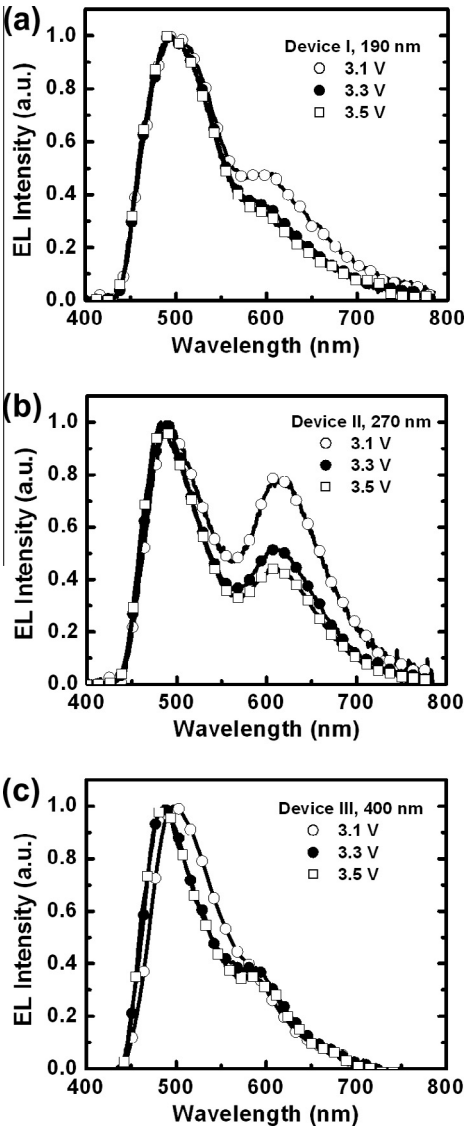

Fig. 5. Stabilized EL spectra of **Device** (a) **I**, (b) **II** and (c) **III** under various biases.

Iterative loops have been carried out for summation of contribution of each emissive sublayer. Based on this simulation method, the simulated output EL spectra of **Device III** when the recombination zone position, as measured from the cathode, varies from 380 to 280 nm are shown in Fig. 4. Simulation of output EL spectra predicts the evolution of measured EL spectra of **Device III** well (*cf.* Figs. 2c and 4), confirming that measured EL spectra resulted from dynamic recombination zone and microcavity effect. Similar evolution of EL spectra has rarely been observed in thinner devices (<200 nm) since the spacing of cavity modes is larger in thinner active layers and significant interference effect would more possibly take place at ultraviolet or near infrared spectral regions, rendering relatively unaffected visible spectra.

The stabilized white EL spectra are bias dependent. As shown in Fig. 5a–c, the relative intensity of the red emission with respect to the blue emission is larger in EL spectra of white LECs under lower biases. Under lower biases, energy level alignments of host and guest (Fig. 1b) favor carrier injection and trapping on the smaller-gap guest, resulting in more red emission. When the bias increases, carrier injection onto the host would be preferred and subsequent energy transfer from host to guest leads to relatively more pronounced blue emission. Furthermore, thicker **Devices II** relatively exhibited more red emission than **Devices I** since a lower electric field in a thick device preferably facilitates carrier trapping effect (*cf.* Fig. 5a and b). However, even thicker **Device III** did not show further enhanced red emission as compared to **Devices I** and **II** (Fig. 5c). It would be attributed that microcavity effect in **Device III** significantly reduces red emission due to destructive interference, eliminating enhanced red emission in a thicker device.

White LECs with various thicknesses showed similar time-dependent EL characteristics under constant-bias operation. Fig. 6a and b shows the time-dependent brightness/current density and EQE/power efficiency, respectively, for **Device II** under constant biases of 3.1–3.5 V. After the bias was applied, the device current, brightness and device efficiency increased due to enhanced carrier injection induced by gradually formed p- and n-type doped layers near electrodes [27]. The brightness and device efficiency first increased with the device current and reached the maximum values. The peak EQEs and the peak power efficiencies of **Device II** at 3.1, 3.3 and 3.5 V are (11.1% and 17.4 lm/W), (10.7% and 19.5 lm/W) and (10.4% and

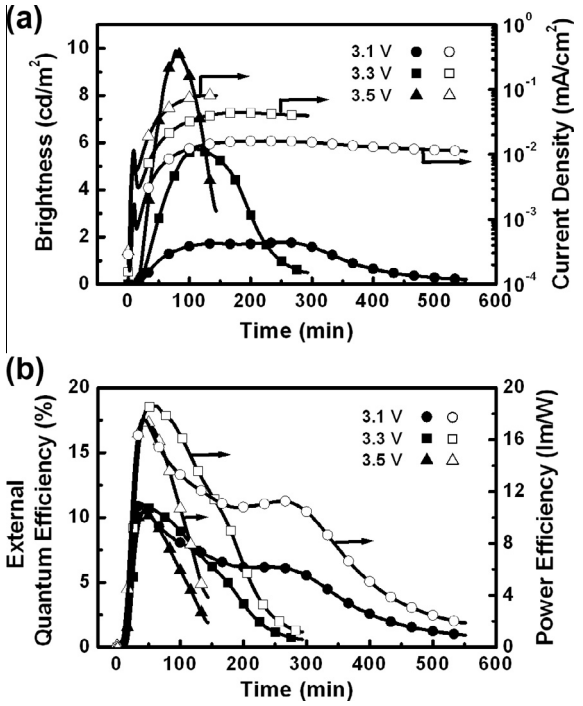

Fig. 6. (a) Brightness (solid symbols) and current density (open symbols) and (b) external quantum efficiency (solid symbols) and power efficiency (open symbols) as a function of time for **Device II** under 3.1–3.5 V.

Table 1
Summary of EL characteristics of white LECs.

Device[a]	Bias (*V*)	CIE (*x*, *y*)[b]	CRI[b]	t_{max} (min)[c]	L_{max} (cd/m^2)[d]	$\eta_{ext,\ max}$, $\eta_{L,\ max}$, $\eta_{p,\ max}$ (%, cd/A, lm/W)[e]	$t_{1/2}$ (min)[f]
I	3.1	(0.305, 0.429)	68	231	3.6	(7.5, 14.5, 14.6)	106
	3.3	(0.274, 0.421)	60	104	8.6	(6.8, 14.0, 13.4)	42
	3.5	(0.266, 0.417)	58	68	14.7	(6.5, 14.5, 13.0)	22
II	3.1	(0.365, 0.401)	77	250	1.8	(11.1, 17.6, 17.4)	110
	3.3	(0.318, 0.386)	74	112	5.7	(10.7, 18.6, 19.5)	89
	3.5	(0.302, 0.376)	73	77	9.9	(10.4, 19.5, 17.5)	57
	5.0	(0.216, 0.400)	44	9	68	(9.0, 18.7, 11.7)	5
	6.0	(0.220, 0.387)	48	7	95	(6.4, 13.4, 7.0)	3
III	3.1	(0.274, 0.485)	40	690	0.5	(4.5, 16.1, 16.3)	146[g]
	3.3	(0.284, 0.401)	61	385	1.4	(4.3, 14.5, 13.8)	87
	3.5	(0.266, 0.404)	55	354	2.4	(4.2, 10.5, 9.5)	55

[a] ITO/PEDOT:PSS (30 nm)/emissive layer/Ag (100 nm), where the emissive layer contains **1** (79.85 wt.%), **2** (0.15 wt.%) and $BMIM^+(PF_6^-)$ (20 wt.%). The thicknesses of the emissive layers for **Device I, II** and **III** are 190, 270 and 400 nm, respectively.
[b] Evaluated from the EL spectra.
[c] Time required to reach the maximal brightness.
[d] Maximal brightness achieved at a constant bias voltage.
[e] Maximal external quantum efficiency, current efficiency and power efficiency achieved at a constant bias voltage.
[f] The time for the brightness of the device to decay from the maximum to half of the maximum under a constant bias voltage.
[g] Extrapolated.

17.5 lm/W), respectively. These results are among the highest reported values for solid-state white LECs [5–9,19,21,22,25,29,32]. Then they dropped with time with a rate depending on the bias voltage (or current). The drop of brightness and device efficiency after reaching the peak value may be associated with exciton quenching near doped layers due to dynamic recombination zone [27] and/or degradation of the emissive material during LEC operation [11].

Low brightnesses of these white LECs result from low device current densities under 3.1–3.5 V. Our previous experimental results show that even with electrochemically doped layers, ohmic contacts (barrier free) for carrier injection could be formed only when carrier injection barriers are relatively lower [36]. For LECs based on complex **1** (Fig. 1a), large injection barriers for hole (~1 eV) and electron (1.2 eV) still result in some residual voltage drops near electrodes since carrier injection layers were shown to significantly enhance device current densities [36]. Therefore, even with much reduced intrinsic layer when the doped layers are well established, device current densities or brightness are still lower under lower biases (3.1–3.5 V). Higher device current densities or brightness can only be obtained under even higher biases.

Higher brightness of LECs can be obtained at the expense of device stability. When the bias voltage is increased to 5 and 6 V, the brightness of white LECs is enhanced to 68 and 95 cd/m^2, respectively (Table 1). However, the device efficiencies and lifetimes under higher voltages deteriorate accordingly (Table 1). To mitigate the device degradation and thus to obtain the best device efficiencies for clarifying the beneficial effect of adopting the strategy of adjusting device thickness, the bias voltages of the white LECs were chosen to be 3.1–3.5 V since the electrochemical band gap of the host material was determined to be 3.08 eV (Fig. 1b). Better device efficiencies can usually be obtained at lower bias voltages (or current densities), as commonly observed in conventional OLEDs [1,2]. Further studies for improving electrochemical stability of the host materials are still required to achieve high device efficiency at adequate brightness for practical applications.

Peak device efficiencies of white LECs are highly thickness dependent (see Table 1). To clarify the physical insight of such phenomenon, the stabilized recombination zone position (z_i, as measured from the cathode) was estimated from fitting of simulated and measured stabilized EL spectra for each white LEC device under 3.5 V. For thinner **Devices I** (190 nm), the stabilized recombination zone was relatively closer to the anode and exciton quenching near the p-type doped layer would lower the device efficiencies [37] (Fig. 7a). Hence, a moderate EQE (7.5%), which is comparable with that of previously reported white LECs based on the same emissive materials in a similar thickness [25], was obtained in **Devices I** (Table 1). Increasing the thickness of the emissive layer would ensure enough spacing between the recombination zone and the doped layers, resulting in mitigated exciton quenching and improved device efficiencies. As shown in Fig. 7b, the stabilized recombination zone of **Device II** (270 nm) was close to the center of the emissive layer and consequently the peak EQE and

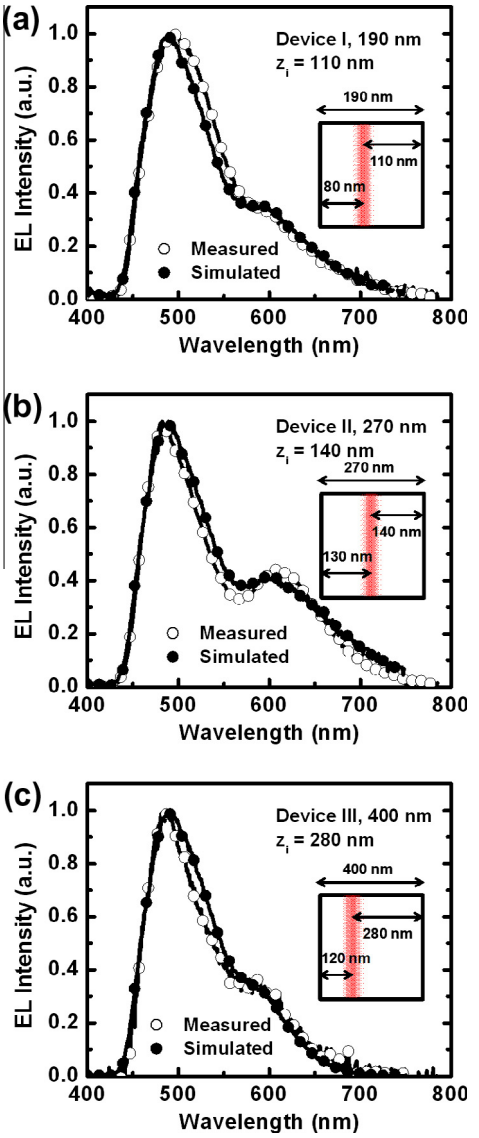

Fig. 7. Simulated (solid symbol) and measured (open symbol) stabilized EL spectra of **Device** (a) **I** (b) **II** and (c) **III** under 3.5 V. The recombination zone position (z_i) estimated from fitting of simulated and measured EL spectra is shown in the inset of each subfigure.

the peak power efficiency were enhanced to *ca.* 11% and 20 lm/W, respectively (Table 1). These device efficiencies are among the highest reported for white LECs [5–9,19,21,22,25,32]. Further increasing the thickness of the emissive layer would not necessarily lead to even higher device efficiencies. For instance, the stabilized recombination zone of thicker **Device III** (400 nm) was rather close to the anode and severe exciton quenching near the p-type doped layer would take place as well. Therefore, significantly deteriorated EQEs (<5%) were measured for **Device III** (Table 1). Highly asymmetric recombination zone position in thicker **Device III** would come from deteriorated balance of carrier mobilities under a lowered electric field. These results confirm that device efficiencies of white LECs could be significantly improved by tailoring the thickness

of the emissive layer to avoid exciton quenching near the doped layers.

4. Conclusions

In summary, we have demonstrated improving device efficiencies of white LECs by optimizing the thickness of the device emissive layer. When the thickness increases from 190 to 270 nm, the recombination zone would be shifted toward the center of the emissive layer and enhanced distance between the recombination zone and doped layers ensures mitigated exciton quenching. Therefore, significant enhancement in device efficiency (1.5×) can be obtained and a high EQE (power efficiency) of *ca.* 11% (20 lm/W) can be achieved. However, further increasing the thickness to 400 nm results in deteriorated balance of carrier mobilities, rendering asymmetric recombination zone position in the emissive layer. Exciton quenching in recombination zone near the doped regions limits device efficiencies as well as that takes place in thinner devices. These results indicate that device efficiencies of white LECs can be optimized by adjusting the thickness of the emissive layer to minimize exciton quenching in close proximity of the doped regions.

Acknowledgement

The authors gratefully acknowledge the financial support from the National Science Council of Taiwan.

References

[1] J. Kido, K. Hongawa, K. Okuyama, K. Nagai, Appl. Phys. Lett. 64 (1994) 815.
[2] B.W. D'Andrade, S.R. Forrest, Adv. Mater. 16 (2004) 1585.
[3] Q. Pei, G. Yu, C. Zhang, Y. Yang, A.J. Heeger, Science 269 (1995) 1086.
[4] Q. Pei, Y. Yang, G. Yu, C. Zhang, A.J. Heeger, J. Am. Chem. Soc. 118 (1996) 3922.
[5] Y. Yang, Q. Pei, J. Appl. Phys. 81 (1997) 3294.
[6] M. Sun, C. Zhong, F. Li, Y. Cao, Q. Pei, Macromolecules 43 (2010) 1714.
[7] S. Tang, J. Pan, H. Buchholz, L. Edman, ACS Appl. Mater. Interfaces 3 (2011) 3384.
[8] C.-S. Tsai, S.-H. Yang, B.-C. Liu, H.-C. Su, Org. Electron. 14 (2013) 483.
[9] S. Tang, J. Pan, H.A. Buchholz, L. Edman, J. Am. Chem. Soc. 135 (2013) 3647.
[10] J.K. Lee, D.S. Yoo, E.S. Handy, M.F. Rubner, Appl. Phys. Lett. 69 (1996) 1686.
[11] G. Kalyuzhny, M. Buda, J. McNeill, P. Barbara, A.J. Bard, J. Am. Chem. Soc. 125 (2003) 6272.
[12] J.D. Slinker, D. Bernards, P.L. Houston, H.D. Abruña, S. Bernhard, G.G. Malliaras, Chem. Commun. (2003) 2392.
[13] K.W. Lee, J.D. Slinker, A.A. Gorodetsky, S. Flores-Torres, H.D. Abruña, P.L. Houston, G.G. Malliaras, Phys. Chem. Chem. Phys. 5 (2003) 2706.
[14] J.D. Slinker, A.A. Gorodetsky, M.S. Lowry, J. Wang, S. Parker, R. Rohl, S. Bernhard, G.G. Malliaras, J. Am. Chem. Soc. 126 (2004) 2763.
[15] A.B. Tamayo, S. Garon, T. Sajoto, P.I. Djurovich, I.M. Tsyba, R. Bau, M.E. Thompson, Inorg. Chem. 44 (2005) 8723.
[16] Q. Zhang, Q. Zhou, Y. Cheng, L. Wang, D. Ma, X. Jing, F. Wang, Adv. Funct. Mater. 16 (2006) 1203.
[17] H.-C. Su, F.-C. Fang, T.-Y. Hwu, H.-H. Hsieh, H.-F. Chen, G.-H. Lee, S.-M. Peng, K.-T. Wong, C.-C. Wu, Adv. Funct. Mater. 17 (2007) 1019.
[18] J.D. Slinker, J. Rivnay, J.S. Moskowitz, J.B. Parker, S. Bernhard, H.D. Abruña, G.G. Malliaras, J. Mater. Chem. 17 (2007) 2976.
[19] H.-C. Su, H.-F. Chen, F.-C. Fang, C.-C. Liu, C.-C. Wu, K.-T. Wong, Y.-H. Liu, S.-M. Peng, J. Am. Chem. Soc. 130 (2008) 3413.
[20] H.J. Bolink, E. Coronado, R.D. Costa, N. Lardiés, E. Ortí, Inorg. Chem. 47 (2008) 9149.
[21] L. He, J. Qiao, L. Duan, G.F. Dong, D.Q. Zhang, L.D. Wang, Y. Qiu, Adv. Funct. Mater. 19 (2009) 2950.
[22] L. He, L. Duan, J. Qiao, G. Dong, L. Wang, Y. Qiu, Chem. Mater. 22 (2010) 3535.
[23] R.D. Costa, E. Ortí, H.J. Bolink, S. Graber, C.E. Housecroft, E.C. Constable, J. Am. Chem. Soc. 132 (2010) 5978.
[24] M. Mydlak, C. Bizzarri, D. Hartmann, W. Sarfert, G. Schmid, L. De Cola, Adv. Funct. Mater. 20 (2010) 1812.
[25] H.-C. Su, H.-F. Chen, Y.-C. Shen, C.-T. Liao, K.-T. Wong, J. Mater. Chem. 21 (2011) 9653.
[26] C.-T. Liao, H.-F. Chen, H.-C. Su, K.-T. Wong, J. Mater. Chem. 21 (2011) 17855.
[27] M. Lenes, G. Garcia-Belmonte, D. Tordera, A. Pertegás, J. Bisquert, H.J. Bolink, Adv. Funct. Mater. 21 (2011) 1581.
[28] C.-T. Liao, H.-F. Chen, H.-C. Su, K.-T. Wong, Phys. Chem. Chem. Phys. 14 (2012) 1262.
[29] H.-B. Wu, H.-F. Chen, C.-T. Liao, H.-C. Su, K.-T. Wong, Org. Electron. 13 (2012) 483.
[30] T. Hu, L. He, L. Duan, Y. Qiu, J. Mater. Chem. 22 (2012) 4206.
[31] R.D. Costa, E. Ortí, H.J. Bolink, F. Monti, G. Accorsi, N. Armaroli, Angew. Chem. Int. Ed. 51 (2012) 8178.
[32] H.-C. Su, H.-F. Chen, P.-H. Chen, S.-W. Lin, C.-T. Liao, K.-T. Wong, J. Mater. Chem. 22 (2012) 22998.
[33] T.-W. Wang, H.-C. Su, Org. Electron. 14 (2013) 2269.
[34] X. Liu, D. Poitras, Y. Tao, C. Py, J. Vac. Sci. Technol. 22 (2004) 764.
[35] I.H. Campbell, D.L. Smith, C.J. Neef, J.P. Ferraris, Appl. Phys. Lett. 72 (1998) 2565.
[36] C.-T. Liao, H.-F. Chen, H.-C. Su, K.-T. Wong, Phys. Chem. Chem. Phys. 14 (2012) 9774.
[37] J. Fang, P. Matyba, L. Edman, Adv. Funct. Mater. 19 (2009) 2671.